

phys. stat. sol. (b) **220**, 417 (2000)

Subject classification: 61.10.Nz; 72.20.Jv; 75.30.Kz; S8.16

Crystallographic, Electrical and Magnetic Properties of the $\text{Cu}_2\text{FeGeSe}_4$ Compound

E. QUINTERO (a), R. TOVAR (a), M. QUINTERO (a), G. SÁNCHEZ-PORRAS (a), P. BOCARANDA (a), J.M. BROTO (b), H. RAKOTO (b), R. BARBASTE (b), J.C. WOOLLEY (c), G. LAMARCHE (c), and A.-M. LAMARCHE (c)

(a) *Centro de Estudios de Semiconductores, Departamento de Física, Facultad de Ciencias, Universidad de Los Andes, Mérida 5101, Venezuela*

(b) *LPMC-SNCMP INSA Complexe Scientifique de Rangueil, F-31077 Toulouse-Cedex, France*

(c) *Ottawa-Carleton Institute for Physics, University of Ottawa, Ottawa, Ontario, K1N 6N5, Canada*

(Received November 1, 1999)

Measurements of X-ray powder diffraction at room temperature, of electrical transport in the temperature range from 100 to 300 K, of magnetic susceptibility χ in the range from 2 to 300 K and of magnetization M as a function of applied magnetic field H at a number of fixed temperatures were made on polycrystalline samples of $\text{Cu}_2\text{FeGeSe}_4$. The analysis of the X-ray diffraction lines show that $\text{Cu}_2\text{FeGeSe}_4$ has the tetragonal stannita structure with lattice parameter values of $a = 5.60078 \text{ \AA}$ and $c = 11.05609 \text{ \AA}$. From the analysis of the electrical data, the values of the hole binding energy E_A and the density of states effective mass of the holes m_p are estimated. The resulting χ vs. T data show that $\text{Cu}_2\text{FeGeSe}_4$ is antiferromagnetic with a Néel temperature $T_N = 20 \text{ K}$ and that a second transition occurs at $\approx 8 \text{ K}$ indicating a transition to weak ferromagnetic state. The magnetization and susceptibility results obtained on $\text{Cu}_2\text{FeGeSe}_4$ show that at all temperatures below $\approx 70 \text{ K}$ bound magnetic polarons (BMPs) occur, in the paramagnetic, antiferromagnetic and weak ferromagnetic ranges. The number of BMPs remained practically constant with temperature having a mean value of $6.55 \times 10^{18} \text{ cm}^{-3}$. Using a simple spherical model, this gives the radius of a BMP as 12.0 \AA .

Introduction Compound semiconductor materials for which an appreciable fraction of the cations are atoms of iron, manganese or similar elements show interesting magnetic properties and all of these materials can be labelled magnetic semiconductors (MS). For MS alloys in which these atoms are at random in the cation lattice, for lower concentrations the material mainly shows spin-glass form, a change to antiferromagnetic form occurring when the concentration exceeds about 0.6 [1]. For compounds, where the arrangement of magnetic atoms on the cation lattice is regular, the exchange between these atoms is usually antiferromagnetic and, in the simplest case, collinear antiferromagnetic behavior occurs. In more recent studies, made of the antiferromagnetic $\text{Cu}_2\text{MnGeS}_4$ compound [2] and also on the $\text{Cu}_2\text{Mn}_{0.9}\text{Zn}_{0.1}\text{SnS}_4$ alloy [3], it was found that the presence of charge carriers (holes in these cases) leads to an indirect Mn–Mn ferromagnetic interaction, i.e. formation of bound magnetic polarons (BMPs) near the occupied acceptors. In these materials, BMPs can arise due to the presence of non-ionized acceptors or donors [4]. The bound hole (electron) interacts with the spins of the magnetic ions within the sphere of its Bohr orbit and tends to produce ferromag-

netic alignment in those spins. Thus, in a simple model, the material can be considered as an irregular assembly of ferromagnetic spheres in a matrix.

In the present work, the crystallographic, electrical and magnetic properties for the compound $\text{Cu}_2\text{FeGeSe}_4$ are studied.

Sample Preparation and Experimental Techniques The polycrystalline samples of $\text{Cu}_2\text{FeGeSe}_4$ used in this work were prepared by the melt and anneal technique, described in detail previously [5]. The X-ray powder diffraction pattern of the sample was recorded at room temperature with a Diffractometer Siemens D5005 equipment using $\text{CuK}\alpha$ ($\lambda = 1.540598 \text{ \AA}$) radiation, to check the equilibrium conditions and to determine lattice parameter values.

The electrical measurements were made on a small slice of about 0.5 mm thickness cut from the $\text{Cu}_2\text{FeGeSe}_4$ ingot used in this work. The conductivity of the sample, as checked by a thermal probe, was found to be p-type. Ohmic electrical contacts to the sample were made by electroplating four symmetrical copper spots, which were used as a base for soldering copper leads with indium. The electrical measurements were made with the van der Pauw method in a magnetic field of 10 kOe. The error in the carrier concentration and mobility measurements was estimated to be about $\pm 5\%$.

Measurements of magnetic susceptibility χ as a function of temperature T in the range 2 to 300 K were made using a Quantum Design SQUID magnetometer with an external magnetic field of 1×10^{-2} T. The resulting variation of χ with T was used to determine the temperatures at which magnetic transitions occurred. The M vs. H measurements at various fixed temperatures were carried out using the SQUID system indicated above, the maximum field in that case being 5 T.

Results and Discussion

X-ray results and analysis The X-ray powder diffraction pattern obtained as indicated above is shown in Fig. 1. The indexing of the diffraction lines was carried out with the computer program DICVOL91 [6] using an absolute error of 0.03° (2θ) in the calculations. The results showed that the $\text{Cu}_2\text{FeGeSe}_4$ compound has the stannite tetragonal structure ($I\bar{4}2m$) and no traces of secondary phases were observed. The obtained lattice parameter values were $a = (5.6008 \pm 0.0004) \text{ \AA}$ and $c = (11.0561 \pm 0.0012) \text{ \AA}$, these

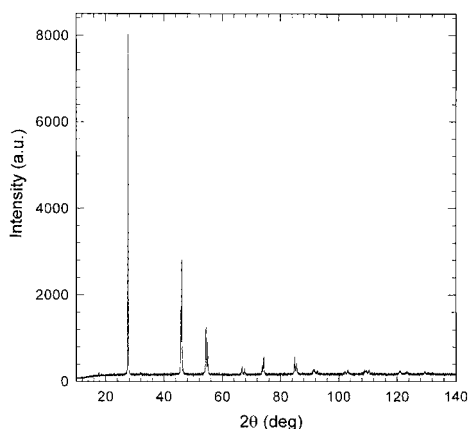


Fig. 1. X-ray diffraction pattern of $\text{Cu}_2\text{FeGeSe}_4$

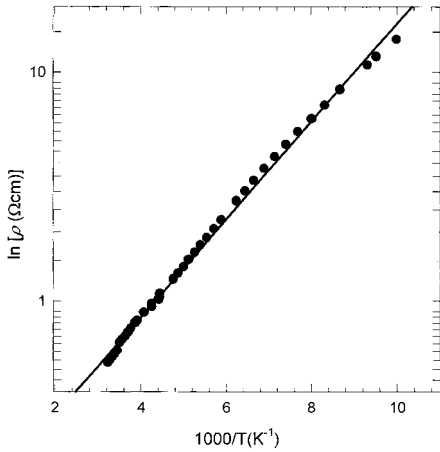


Fig. 2. Variation of resistivity ρ with $1000/T$ for $\text{Cu}_2\text{FeGeSe}_4$

results are in good agreement with those reported by Schäfer and Nitsche [7].

Resistivity and hole concentration The resistivity ρ was measured in the temperature range from 100 to 300 K and the resulting $\log(\rho)$ vs. $1000/T$ curve is shown in Fig. 2. The hole binding energy E_A was estimated from the slope of this curve, and the resulting value was found to be $E_A \approx 42$ meV, with an uncertainty of about 10%.

The variation of the hole concentration p vs. T is shown in Fig. 3. To get an estimate of the activation energy E_A of the acceptor level and the density states effective mass m_p , the temperature dependence of the hole concentration was analyzed using the following expression for nondegenerate statistic of a single level [8]:

$$\frac{p(p + N_d)}{(N_a - N_d - p)} = \frac{2(2\pi m_p kT/h^2)^{3/2}}{\beta} \exp(-E_A/kT), \quad (1)$$

where N_a and N_d are the acceptor and compensating donor densities, respectively, and β is the impurity degeneracy, which is, taken to be 2 in the present case. The criteria used to determine these parameters were to choose values of N_a and N_d until a linear plot of

$$\ln \left[p(p + N_d)/(N_a - N_d - p) T^{3/2} \right] \text{ vs. } 1000/T \quad (2)$$

including the maximum number of experimental points was obtained. Then a linear least-square fit to these points was carried out. The activation energy E_A estimated from the slope of that line was found to be (43.4 ± 1.4) meV. This value is very close to the one obtained from the resistivity data in Fig. 2. The resulting values of N_a and N_d were $2 \times 10^{19} \text{ cm}^{-3}$ and $1 \times 10^{18} \text{ cm}^{-3}$, respectively. The density of states effective mass m_p value determined from the intercept at $T \rightarrow \infty$ was found to be $1.32 m_0$.

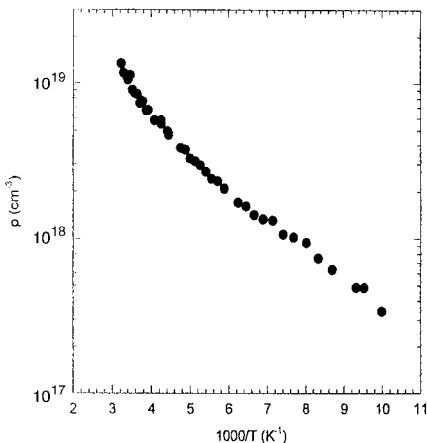


Fig. 3. Variation of hole concentration p with $1000/T$ for $\text{Cu}_2\text{FeGeSe}_4$

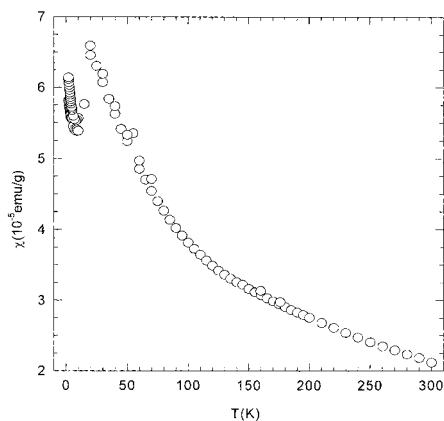


Fig. 4. Variation of magnetic susceptibility as a function of temperature T for $\text{Cu}_2\text{FeGeSe}_4$

Magnetic results and discussion Curves of χ vs. T and $1/\chi$ vs. T are shown in Figs. 4 and 5, respectively. From Fig. 4, it is seen that magnetic transitions occur at temperatures of about 20 K and 8 K. The one at 20 K is typical of an antiferromagnetic material, while the lower one has the form associated with a ferromagnetic transition. For antiferromagnetic behavior, the variation of $1/\chi$ with T well above the Néel temperature is

given by the relation $1/\chi = (T - \theta)/C$, where θ is the Curie-Weiss temperature and C the Curie constant. The experimental data for $T \geq 100$ K shown in Fig. 5 were fitted to the above equation. The resulting values of C and θ were 9.8973×10^{-3} emuK/g and -159.737 K, respectively. Below 100 K, the deviation from linearity indicates the occurrence of another magnetic effect, as indicated below, this deviation is due to the presence of free carriers, which could lead to the formation of BMPs [3, 4, 9].

For the magnetization measurements, in all cases the M vs. H data showed the general form expected when BMPs are present in the compound, and a set of M vs. H results, for values of H up to 5 T, are shown in Fig. 6. Here, the experimental points are shown with curves determined by fitting to eq. (3) as discussed below. For temperatures below 20 K, the curves are close together and some overlap occurs. This behavior can be attributed to effects of anisotropy at low temperatures. From the form of the M vs. H curves in Fig. 6, it is seen that the magnitude of the BMP resultant moment falls with increasing temperature, becoming practically zero at 77 K. At high temperatures, the compound shows normal paramagnetic form, but in the vicinity of 80 K, BMPs are observed in a paramagnetic matrix. As seen from the χ vs. T curve, a transition to antiferromagnetic form occurs at the Néel temperature $T_N = 20$ K and below this the BMPs occur in this antiferromagnetic matrix. Finally below 8 K, the BMPs are present, but a weak ferromagnetic behaviour also occurs.

As has been shown previously [3], the M vs. H curves for BMPs can be very well fitted to an equation of the form

$$M = Nm_s L(x) + \chi_m H, \quad (3)$$

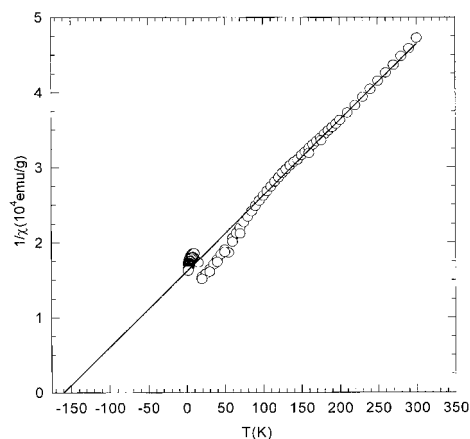


Fig. 5. Variation of $1/\chi$ as a function of temperature T for $\text{Cu}_2\text{FeGeSe}_4$

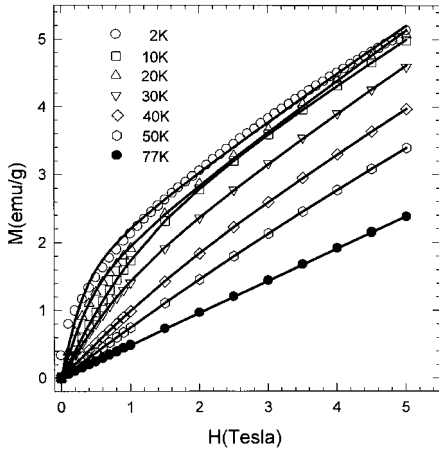


Fig. 6. Variation of magnetization M as a function of applied field H for a range of temperatures for $\text{Cu}_2\text{FeGeSe}_4$

Table 1
Values of the fitting parameters of BMPs as a function of temperature

T (K)	Nm_s (emu/g)	χ_m (10^{-5} emu/g)	m_{eff} (μ_B)	Nm_s/m_{eff} (emu/ μ_B g)	Nm_s/N (μ_B)
2	1.2070	7.956	29.6241	0.0407	109.7273
5	1.8193	6.7089	19.0826	0.0953	165.3909
10	1.9596	6.7089	31.2376	0.0627	178.1455
16	1.6989	6.864	68.7729	0.0247	154.4455
20	1.5076	7.3526	146.6989	0.0103	137.0545
30	1.2192	6.9743	105.5623	0.0115	110.8364
40	0.8636	6.4534	78.2718	0.0110	78.5091
50	0.5611	5.9069	63.5970	0.0088	51.0091

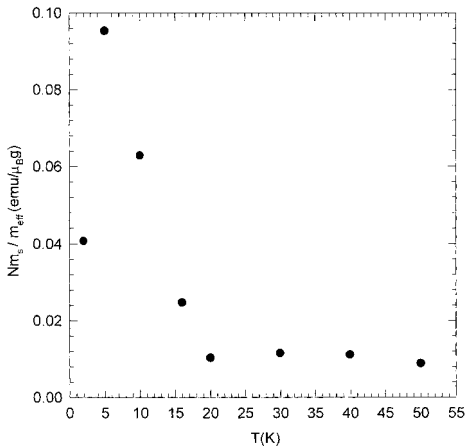


Fig. 7. Variation of Nm_s / m_{eff} with temperature T for $\text{Cu}_2\text{FeGeSe}_4$

where the Langevin term $L(x) = (\coth x - 1/x)$ represents the contribution of BMPs and the term $\chi_m H$ the contribution of the matrix. Here, $x = m_{\text{eff}} H / k_B T$, where N is the number of BMPs involved, m_s and m_{eff} are, respectively, the true and effective spontaneous moments per BMP. In the Langevin function, the effective moment m_{eff} determines how quickly the true moment aligns along H . Because of the effects of interaction between the BMPs, Wolff (quoted in [3]) has proposed that $m_{\text{eff}} = m_s T / (T + T')$, where T' represents the interaction. With T' relatively small, at the higher temperatures investigated, to a good approximation $m_{\text{eff}} = m_s$. As was shown by McCabe et al. [3], for temperatures lower than ≈ 20 K, anisotropy behavior is observed. Thus at a given T , the values of M are different for H parallel and H perpendicular to the symmetry axis c . However, for temperatures above about 20 K, the anisotropy effects were found to be negligible, and in this range $m_{\text{eff}} = m_s$. So that the effects of anisotropy will be important only in the antiferromagnetic range. As indicated above, the fitted curves are shown in Fig. 6, where it is seen that in most cases a very good fit was obtained. Values of the fitting parameters were thus determined as a function of temperature, and these are listed in Table 1. As indicated by McCabe et al. [3], in the range where $m_s = m_{\text{eff}}$, values for N can be obtained from the ratio Nm_s/m_{eff} . In Fig. 7, values are shown for Nm_s/m_{eff} ($= N$) as a function of T . It is seen that in the range $20 \text{ K} < T < 50 \text{ K}$, this value is almost constant with a mean value of 0.011 g^{-1} , i.e. N is almost constant with a mean value in this temperature range of $0.011 \mu_B \text{ g}^{-1} = 1.19 \times 10^{18} \text{ g}^{-1}$. This gives a value of N and hence a concentration of non-ionized acceptors of $6.55 \times 10^{18} \text{ cm}^{-3}$. With this value for N , values for m_s can be obtained from the Nm_s values and the variation of m_s with T is shown in Fig. 8. It is seen that for 10 K and above the variation of m_s with T is practically linear, and extrapolates to a value of $212 \mu_B/\text{BMP}$ at $T = 0$. Taking the atomic moment for Fe^{2+} as $5 \mu_B$, this gives the mean number of Fe atoms in each BMP as 42.4. This is to be compared with the value of 28.6 Mn ions per BMP obtained by McCabe et al. [3] for p-type $\text{Cu}_2\text{Mn}_{0.9}\text{Zn}_{0.1}\text{SnS}_4$. Assuming in a very simple model, that all Fe ions inside a spherical BMP are aligned and none outside contribute, this gives the radius of the BMP to be 12.0 \AA , which is a reasonable number for an acceptor Bohr radius in such a material.

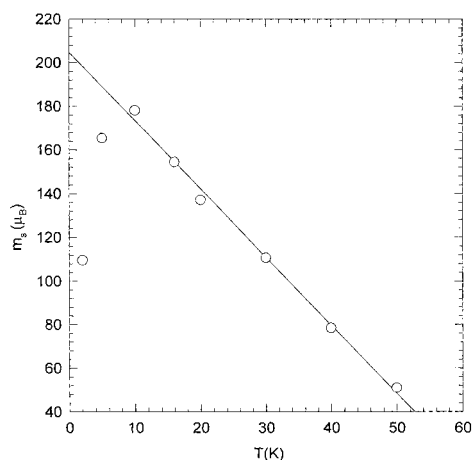


Fig. 8. Variation of m_s with temperature T for $\text{Cu}_2\text{FeGeSe}_4$

References

- [1] J.C. WOOLLEY, S.F. CHEHAB, T. DONOFRIO, S. MANHAS, G. LAMARCHE, and A. MANOOGIAN, *J. Magn. Magn. Mater.* **61**, 13 (1986).
- [2] Y. SHAPIRA, E.J. MCNIFF, JR., N.F. OLIVEIRA, JR., E.D. HONIG, K. DWIGHT, and A. WOLD, *Phys. Rev. B* **37**, 411 (1988).
- [3] G.H. MCCABE, T. FRIES, M.T. LIU, Y. SHAPIRA, L.R. RAM-MOHAN, R. KERSHAW, A. WOLD, C. FAU, M. AVEROUS, and N.F. MCNIFF, JR., *Phys. Rev. B* **56**, 6673 (1997).
- [4] P.A. WOLFF, *Diluted Magnetic Semiconductors*, Ed. J.K. FURDYNA and J. KOSSUT, *Semiconductors and Semimetals*, Vol. 25, Academic Press, New York 1988.
- [5] M. QUINTERO, A. BARRETO, P. GRIMA, R. TOVAR, E. QUINTERO, G. SÁNCHEZ-PORRAS, J. RUIZ, J.C. WOOLLEY, G. LAMARCHE, and A.-M. LAMARCHE, *Mater. Res. Bull.*, accepted for publication.
- [6] A. BOULTIF and D. LOUER, *J. Appl. Cryst.* **24**, 987 (1980).
- [7] W. SHÄFER and R. NITSCHKE, *Mater. Res. Bull.* **9**, 645 (1974).
- [8] J.S. BLAKEMORE, *Solid State Physics*, Saunder, Toronto 1974.
- [9] J.K. FURDYNA and J. KOSSUT, *Diluted Magnetic Semiconductors, Semiconductors and Semimetals*, Eds. R.K. WILLARDSON and A.C BEER, Academic Press, New York 1988 (Vol. 25, Chap. 1).

